Electroreflectance in a Nonuniform Field in the Small-Wave-Number Approximation and Its Measurement by Ellipsometry

E. Yang* and A. B. Buckman
Electrical Materials Laboratory, Department of Electrical Engineering, University of Nebraska, Lincoln, Nebraska 68508
(Received 9 February 1970; revised manuscript received 27 August 1971)

The changes in the real and imaginary parts of the dielectric constant of a solid induced by an electric field which decreases exponentially with distance from the surface are calculated from perturbation theory for photon energies near interband transitions. This exponential model for the field is of interest because it approximates well the actual field over a fairly wide range of surface conditions and because it contains only two adjustable parameters, the surface field and the rate of decay of the exponential. The contribution from each of these parameters can be separated and identified in the results. Previous calculations of electroreflectance in a nonuniform field have employed the one-electron Franz-Keldysh theory for a uniform field, assuming the field to vary slowly enough with distance from the surface so that a WKB approximation could be used to extract spatially averaged values of the change in dielectric constant. Our calculation is not limited by the WKB approximation, and is applicable even at very large field nonuniformities. However, when the field penetration depth is less than about three times the photon penetration depth, effective masses must be known in order to complete our calculation, but it is still valid. The theory, used to interpret a modulated-ellipsometry experiment on Ge in the 2.1-eV region, shows that illumination of the sample surface by a second light beam can decrease the field penetration depth by at least a factor of 20, and increase the surface field by at least a factor of 10, because of increased free-carrier screening.

I. INTRODUCTION

The effect of spatial inhomogeneity in the dielectric-constant perturbations $\delta\epsilon_1$ and $\delta\epsilon_2$ on electroreflectance spectra has been the subject of a number of recent investigations.[1-5] In these papers the approach has been to calculate $\delta\epsilon_1$ and $\delta\epsilon_2$ using the one-electron Franz-Keldysh theory for a uniform electric field,[6,7] assuming that the field varies slowly enough with depth so that the uniform-field theory is applicable, and then to construct spatially dependent functions for $\delta\epsilon_1$ and $\delta\epsilon_2$, from which either the expected electroreflectance signal or spatially averaged dielectric-constant perturbations can be calculated and compared with experiment.

However, criteria for how slowly the field must vary with depth in order for this approach to be valid have not been established. Aspnes and Frova,[5] in a calculation based on the WKB approximation, have considered only the variation of $\delta\epsilon_1$ and $\delta\epsilon_2$ over the depth penetrated by the light incident on the sample, and have solved Maxwell's equations for an inhomogeneous medium to derive spatially averaged perturbations which can be used to calculate electroreflectance spectra.

In this paper, a different approach is taken. The primary emphasis in the calculation is on the nonuniformity of the electric field rather than that of $\delta\epsilon_1$ and $\delta\epsilon_2$. When the distance λ_p over which $\delta\epsilon_1$ and $\delta\epsilon_2$ vary significantly becomes shorter than the light wavelength, another approximation may be made instead, the small-wave-number approximation as discussed by Jacobsson,[8] Drude,[9] and Rayleigh.[10] In this case the variation of $\delta\epsilon_1$ and $\delta\epsilon_2$ over $0 \leq x \leq \lambda_p$ is replaced by an average value over the same distance. This is the case treated by our calculation. The nonuniformity of the electric field is retained in the quantum-mechanical calculation of $\delta\epsilon_1$ and $\delta\epsilon_2$, but the complicated nonuniformity in $\delta\epsilon_1$ and $\delta\epsilon_2$ is replaced by a surface film with perturbed dielectric constants overlaying a bulk sample whose dielectric constants are unperturbed. Therefore, for measurements in the visible spectrum, with the wavelength λ of the order of thousands of Å, our model should be applicable for samples with carrier densities large enough to reduce λ_p to the order of 10^3 Å or less.

It should be emphasized that since the dependence of $\delta\epsilon_1$ and $\delta\epsilon_2$ on the electric field is nonlinear, λ_p will generally not be the same as the penetration depth of the electric field. However, as will be seen later, λ_p does not enter the theoretical calculation of $\delta\epsilon_1$ and $\delta\epsilon_2$ directly, but affects only the determination of $\delta\epsilon_1$ and $\delta\epsilon_2$ from experimental data. This effect of λ_p on the experimental values of $\delta\epsilon_1$ and $\delta\epsilon_2$ has been pointed out earlier.[11]

A surface electric field profile of the form $\mathcal{E} = \mathcal{E}_0 e^{-\alpha x}$ is chosen for the theoretical calculation since it approximates well the actual field profile over a fairly wide range of surface conditions, contains only two adjustable parameters, $\mathcal{E}_0$ and α, and yields theoretical spectra which allow contributions from changes in $\mathcal{E}_0$ and α to be separately

identified.

Several workers have attributed observed photoreflectance in semiconductors to the electroreflectance mechanism arising from changes in the surface electric field profile owing to the photoexcited electron-hole pairs.[12–14] It is of interest to measure these changes experimentally. Aspnes[14] has obtained the surface electric fields in his photoreflectance experiments on Ge by high-speed capacitance measurements. Changes with photoexcitation in both the surface electric field and the free-carrier screening depth can be obtained optically from our ellipsometric experiment.

II. THEORY

The approach taken here is to find the eigenfunctions and eigenvalues for a solid subject to a spatially dependent potential $f(x)$ from perturbation theory, and to use these in the standard expression for the total transition probability

$$W_{\text{tot}} = \frac{2\pi e^2 A^2}{m^2 c^2 \hbar N^2} \sum_{\substack{\nu,\nu',n,n',\\ \vec{k},k_x'}} \hat{\epsilon}\cdot P_{n',n}(\vec{k}_\perp,k_x)\,\hat{\epsilon}\cdot P^*_{n',n}(\vec{k}_\perp,k_x') \times A^*_{\nu',n'}(\vec{k}_\perp,k_x) A_{\nu,n}(\vec{k}_\perp,k_x) A^*_{\nu,n}(\vec{k}_\perp,k_x') A_{\nu',n'}(\vec{k}_\perp,k_x') \times \delta(W_{\nu',n'}(\vec{k}_\perp) - W_{\nu,n}(\vec{k}_\perp) - \hbar\omega)\,, \quad (1)$$

where $\vec{k}_\perp$ is the momentum vector perpendicular to the direction of spatial variation, i.e., perpendicular to the applied electric field, k_x is the momentum vector in the direction of the electric field, here assumed not conserved, $\hat{\epsilon}\cdot P_{n',n}(\vec{k}_\perp,k_x)$ are analogous to the quantities used by Aspnes, Handler, and Blossey,[6] and the sum n' ranges over all filled bands and n over all empty bands. The eigenfunctions in the presence of the x-dependent potential are expanded as

$$\phi_{\nu,n}(\vec{k},\vec{r}) = \sum_{k_x} A_{\nu,n}(\vec{k})\,\psi_n(\vec{k},\vec{r})\,, \quad (2)$$

where the ψ_n are the Bloch functions. The $W_{\nu,n}(\vec{k}_\perp)$ are the eigenvalues in the presence of the field.

A perturbing electric field of the form $\mathcal{E} = \mathcal{E}_0 \times e^{-\alpha x}$ has been used, and the perturbations on ψ_n, because of the termination of the lattice at the surface, have been neglected. The $A_{\nu,n}$ and $W_{\nu,n}$ for this case are calculated from perturbation theory in the Appendix with $f(x) = B(1-e^{-\alpha x})$, where $B = -e\mathcal{E}_0/\alpha$.

Substitution of the $A_{\nu,n}$ and $W_{\nu,n}$ into (1) yields

$$W_{\text{tot}} = \frac{2e^2A^2}{m^2c^2\hbar N^2} \sum_{\substack{\nu,\nu',n,n',\\ \vec{k},k_x'}} \hat{\epsilon}\cdot P_{n',n}(\vec{k})\,\hat{\epsilon}\cdot P^*_{n',n}(\vec{k})\, e^{-\bar{\Delta}(k_x,k_x')} \exp\left[\frac{i}{\alpha}\int_{k_x'}^{k_x} \ln\left(\frac{E_n(k,q_x') - \bar{E}_n(\vec{k}_\perp) + Be^{\theta}e^{-2\pi\nu\alpha/K_x}}{E_n'(\vec{k}_\perp,q_x') - \bar{E}_{n'}(\vec{k}_\perp) + Be^{\theta'}e^{-2\pi\nu'\alpha/K_x}}\right) dq_x'\right] \times \delta(-Be^{\theta}e^{-2\pi\nu\alpha/K_x} + Be^{\theta'}e^{-2\pi\nu'\alpha/K_x} + \bar{E}_{n,n'}(\vec{k}_\perp) - \hbar\omega)\,, \quad (3)$$

where

$$\bar{E}_{n,n'}(\vec{k}_\perp) = \bar{E}_n(\vec{k}_\perp) - \bar{E}_{n'}(\vec{k}_\perp)\,, \quad \bar{E}_n(\vec{k}_\perp) = E_n(\vec{k}_\perp) + \frac{\hbar^2}{2\mu_x}K_X^2 \text{ (effective-mass approx.)}\,, \quad \bar{\Delta}(k_x,q_x) = \int_{q_x}^{k_x}\Delta(\vec{k}_\perp,k_x)\,dk_x\,,$$

$$\Delta(k_x,q_x) = \int_{q_x}^{k_x}[\delta_{kk'}\bar{X}_{nn'}(\vec{k}) - X_{nn}(\vec{k})]\,dk_x'\,, \quad \bar{X}_{nn'}(\vec{k}) = \begin{cases} X_{nn'}(\vec{k}) & \text{if } n\neq n' \\ 0 & \text{if } n = n' \end{cases}\,, \quad X_{nn'}(\vec{k}) = \langle\psi_{n'}(\vec{k},\vec{r})\,|\,x\,|\,\psi_n(\vec{k},\vec{r})\rangle\,, \quad (4)$$

and θ and θ' are defined in the Appendix.

To calculate the sum over ν and ν', let

$$f(\nu,\nu') = \frac{1}{N}\exp\left[\frac{i}{\alpha}\int_{k_x'}^{k_x}\ln\left(\frac{E_n(\vec{k}_\perp,q_x') - \bar{E}_n(\vec{k}_\perp) + Be^{\theta}e^{-2\pi\nu\alpha/K_x}}{E_{n'}(\vec{k}_\perp,q_x') - \bar{E}_{n'}(\vec{k}_\perp) + Be^{\theta'}e^{-2\pi\nu'\alpha/K_x}}\right)dq_x'\right] \times \delta(-Be^{\theta}e^{-2\pi\nu\alpha/K_x} + Be^{\theta'}e^{-2\pi\nu'\alpha/K_x} + \bar{E}_{nn'}(\vec{k}_\perp) - \hbar\omega)\,. \quad (5)$$

The indices ν, ν' range over the integers 0 to N, where N is very large, and f decreases with increasing ν or ν'. Therefore, the sum in (5) can be replaced by an integral,

$$\sum_{\nu\nu'} f(\nu,\nu') = \int_0^{N\to\infty}\int_0^{N\to\infty} f(\nu,\nu')\,d\nu\,d\nu'\,. \quad (6)$$

Substituting Eq. (6) into Eq. (3) and integrating over ν yields

$$\sum_{\nu\nu'} f(\nu,\nu') = \frac{1}{N}\int_0^{N\to\infty}\frac{K_x}{2\pi}\frac{1}{\alpha}\left|Be^{\theta'}e^{-2\pi\nu'\alpha/K_x} + \bar{E}_{nn'}(\vec{k}_\perp) - \hbar\omega\right|^{-1}$$

$$\times\exp\left[\frac{1}{\alpha}\int_{k_x'}^{k_x}\ln\left(\frac{E_n(\vec{k}_\perp,q_x)-\bar{E}_n'(\vec{k}_\perp)+Be^{\theta'}e^{-2\pi\nu'\alpha/K_x-\hbar\omega}}{E_{n'}(\vec{k}_\perp,q_x)-\bar{E}_{n'}(\vec{k}_\perp)+Be^{\theta'}e^{-2\pi\nu'\alpha/K_x}}\right)dq_x\right]d\nu' , \quad (7)$$

where we have used

$$\delta(f(x))=\left(\left|\frac{df(x)}{dX}\right|_{X_{f(x)=0}}\right)^{-1}\delta(X-X_{f(x)=0}) .$$

To carry out the second sum over ν', let $2\pi\nu'/K_x=l$. Then Eq. (7) becomes

$$\sum_{\nu\nu'}f(\nu,\nu')=\frac{K_x}{2\pi}\frac{1}{\alpha}\frac{1}{L_x}\int_0^{L_x}[Be^{\theta'}e^{-l\alpha}+\bar{E}_{nn'}(\vec{k}_\perp)-\hbar\omega]^{-1}\exp\left[\frac{i}{\alpha}\int_{k_x'}^{k_x}\ln\left(\frac{E_n(\vec{k}_\perp,q_x)-\bar{E}_n'(\vec{k}_\perp)+Be^{\theta'}e^{-l\alpha}-\hbar\omega}{E_n'(\vec{k}_\perp,q_x)-\bar{E}_n'(\vec{k}_\perp)+Be^{\theta'}e^{-l\alpha}}\right)dq_x\right]dl , \quad (8)$$

where $L_x=Nd$, d is the lattice constant in x direction, and $K_x=2\pi/d$. The quantity L_x can be interpreted as the effective "length of the sample" in the x direction. For a reflection experiment, this is just the penetration depth of the photons. Substituting Eq. (8) into Eq. (3), we have the imaginary part of the dielectric function[6] (BZ is the Brillouin zone)

$$\epsilon_2(\omega,\mathcal{E})=\sum_{n,n'}\frac{2\pi e^2}{m^2\omega^2}\frac{1}{L_x\alpha}\int_0^{L_x}dl\,\frac{2}{(2\pi)^3}\int_{BZ}dk\int_{BZ}dk_x\int_{BZ}dk_x'\,|\hat{\epsilon}\cdot P_{nn'}|^2\,|[Be^{\theta'}e^{-l\alpha}+\bar{E}_{nn'}(\vec{k}_\perp)-\hbar\omega]|^{-1}$$

$$\times\exp\left[\frac{i}{\alpha}\int_{k_x'}^{k_x}\ln\left(\frac{E_n(\vec{k}_\perp,q_x)-\bar{E}_n'(\vec{k}_\perp)+Be^{\theta'}e^{-l\alpha}-\hbar\omega}{E_n'(\vec{k}_\perp,q_x)-\bar{E}_n'(\vec{k}_\perp)+Be^{\theta'}e^{-l\alpha}}\right)dq_x\right] . \quad (9)$$

At this point it is appropriate to consider only one interband transition between band n and n', and change variables of integration as in Ref. 6. Equation (9) can then be rewritten as

$$\epsilon_2(\omega,\mathcal{E})=\frac{4\pi e^2}{\omega^2m^2}\frac{1}{L_x}\int_0^{L_x}\frac{2}{(2\pi)^3}\int_{BZ}d^3k\,\frac{|\hat{\epsilon}\cdot P_{nn'}|^2}{|e^{-l\alpha}-(\alpha/e\mathcal{E}_0)[E_{nn'}(\vec{k}_\perp)-\hbar\omega]|}$$

$$\times\int_{-\infty}^{\infty}db\exp\left[\frac{ie\mathcal{E}_0}{\alpha}\int_{-b}^{b}\ln\left(\frac{E_n(\vec{k}+te\mathcal{E}_0)-E_n'(\vec{k}_\perp)+Be^{-\alpha l}-\hbar\omega}{E_{n'}(\vec{k}+te\mathcal{E}_0)-\bar{E}_n'(\vec{k}_\perp)+Be^{-\alpha l}}\right)dt\right] , \quad (10)$$

where we have used the weak-field approximation which leads to

$$e^{-\theta'}\approx 1, \quad \Delta(k_x,k_x')\approx 0 ,$$

and

$$P_{nn'}(\vec{k}+be\mathcal{E}_0)=P_{nn'}(\vec{k}-be\mathcal{E}_0)=P_{nn'}(\vec{k}) .$$

To obtain an expression in terms of the surface field $\mathcal{E}_0$ which has a form that can be reduced to the case of zero field, we expand the energy term in Eq. (10) in terms of the surface field

$$\ln f(\vec{k}+et\mathcal{E}_0)=\ln f(\vec{k})+t\frac{(e\mathcal{E}_0\cdot\nabla_{\vec{k}})E_n(\vec{k})}{f(\vec{k})}$$

$$+\frac{t^2}{2}\left[\frac{(e\mathcal{E}_0\cdot\nabla_{\vec{k}})^2E_n(\vec{k})}{f(\vec{k})}+\left(\frac{[e\mathcal{E}_0\cdot\nabla_{\vec{k}}E_n(\vec{k})]}{f(\vec{k})}\right)^2\right]+\cdots , \quad (11)$$

where $f(\vec{k}+te\mathcal{E}_0)$ stands for

$$E_n(\vec{k}+te\mathcal{E}_0)-\bar{E}_n'(\vec{k}_\perp)+Be^{-l\alpha}-\hbar\omega .$$

A similar expression can be derived for

$$\ln[E_{n'}(\vec{k}+te\mathcal{E}_0)-\bar{E}_{n'}(\vec{k}_\perp)+Be^{-\alpha l}] .$$

Substituting Eq. (11) in Eq. (10), we have

$$\epsilon_2(\omega,\mathcal{E})=\frac{4\pi e^2}{\omega^2m^2}\frac{1}{L_x}\int_0^{L_x}dl\,\frac{2}{(2\pi)^3}\int_{BZ}d^3k\,\frac{|\hat{\epsilon}\cdot P_{nn'}'|^2}{|e^{-l\alpha}-(\alpha/e\mathcal{E}_0)[\bar{E}_{nn'}(\vec{k}_\perp)-\hbar\omega]|}$$

$$\times\int_{-\infty}^{\infty}db\exp\left\{\frac{ie\mathcal{E}_0}{\alpha}\left[2b\ln\left(\frac{E_n(\vec{k})-\bar{E}_n'(\vec{k}_\perp)+Be^{-\alpha l}-\hbar\omega}{E_n'(\vec{k})-\bar{E}_n'(\vec{k}_\perp)+Be^{-\alpha l}}\right)\right]-i\frac{b^3}{3}[Y(k,\alpha)]^3\right\} , \quad (12)$$

where

$$[Y(k,\alpha)]^3 = \frac{e\mathcal{E}_0}{\alpha}\left[\frac{(e\mathcal{E}_0\cdot\nabla_{\vec{k}})^2 E_n(\vec{k})}{E_n(\vec{k})-\bar{E}_{n'}(\vec{k}_\perp)+Be^{-\alpha l}-\hbar\omega}+\frac{(e\mathcal{E}_0\cdot\nabla_{\vec{k}})^2 E_n'(\vec{k})}{E_n'(\vec{k})-\bar{E}_{n'}(\vec{k}_\perp)+Be^{-\alpha l}}\right.$$
$$\left.+\left(\frac{(e\mathcal{E}_0\cdot\nabla_{\vec{k}})E_n'(\vec{k})}{E_n'(\vec{k})-\bar{E}_{n'}(\vec{k}_\perp)+Be^{-\alpha l}}\right)^2+\left(\frac{(e\mathcal{E}_0\cdot\nabla_{\vec{k}})E_n(\vec{k})}{E_n(\vec{k})-\bar{E}_n'(\vec{k}_\perp)+Be^{-\alpha l}-\hbar\omega}\right)^2\right]. \quad (13)$$

The odd terms in electric field have been removed by integration over the variable t and thus the next-higher-order term, which is fourth order in the electric field, is assumed to be negligible.

Equation (12) can be expressed in terms of the Airy function as

$$\epsilon_2(\omega,\mathcal{E}) = \frac{4\pi^2e^2}{\omega^2m^2}\frac{1}{L_x}\int_0^{L_x} dl\,\frac{2}{(2\pi)^3}\int_{BZ} d^3k\,\frac{|\hat{\epsilon}\cdot P_{nn'}|^2}{|e^{-l\alpha}-(\alpha/e\mathcal{E}_0)[\bar{E}_{nn'}(\vec{k}_\perp)-\hbar\omega]|}$$
$$\times\frac{1}{\frac{1}{2}Y(\vec{k},\alpha)}\,\mathrm{Ai}\left[\frac{2e\mathcal{E}_0}{\alpha}\ln\left(\frac{E_n(\vec{k})-\bar{E}_{n'}(\vec{k}_\perp)+Be^{-\alpha l}-\hbar\omega}{E_n'(\vec{k})-\bar{E}_{n'}(\vec{k}_\perp)+Be^{-\alpha l}}\right)\Big/Y(\vec{k},\alpha)\right], \quad (14)$$

where

$$\mathrm{Ai}(x) = \frac{1}{2\pi}\int_{-\infty}^{\infty} e^{-iS^3/3-iSx}\,dS\,. \quad (15)$$

As $\alpha\to 0$, we have

$$\lim_{\alpha\to 0}\epsilon_2(\omega,\mathcal{E}) = \frac{4\pi^2e^2}{m^2\omega^2}\int_{BZ} d^3k\,|\hat{\epsilon}\cdot P_{n'n}|^2$$
$$\times\frac{1}{|\hbar\Omega|}\,\mathrm{Ai}\left(\frac{E_{n'n}(\vec{k})-\hbar\omega}{\hbar\omega}\right), \quad (16)$$

the same results as those derived by Aspnes, Handler, and Blossey[6] for a uniform electric field.

Comparison of (14) and (16) shows that the effect of the field nonuniformity is to replace the Airy-function line shape of the uniform-field calculation by an integrated Airy function multiplied by a normalizing prefactor.

For regions of k space near critical points, the effective-mass approximation can be used, and the spectra for $\delta\epsilon_2$ can be calculated by subtracting the zero-field values of $\epsilon_2(\omega,0)$ from (14). The Kramers-Kronig analysis can then be used to calculate $\delta\epsilon_1$ for each $\delta\epsilon_2$ spectrum. These line shapes have been calculated numerically.

Just as in the uniform-field case, two characteristic line shapes are obtained. These are labeled $X(\Lambda)$ and $Y(\Lambda)$ and are shown in Figs. 1 and 2, respectively, for different degrees field nonuniformity. If we define the electric field penetration depth $L_D = 1/\alpha$, the most convenient measure of field nonuniformity for a reflection experiment is the ratio L_x/L_D. If this ratio is small, the reflected photons sample only a very small part of the total variation of the electric field with distance, resulting in spectra almost exactly the same as those for a uniform field. Conversely, if this ratio is large, the photons sample all values of the electric field from $\mathcal{E}_0$ to very nearly zero, greatly modifying the line shapes.

Just as with the uniform-field theory, the signs of X, Y, and the argument Λ appear in different combinations for different types of critical points. The correct relationships are given in Table I.

Inspection of the curves in Figs. 1 and 2 reveals the following important characteristics: (i) The ratio of the height of any satellite peak to the main-peak height of any structure is a function of L_x/L_D only, and is independent of $\mathcal{E}_0$. (ii) Therefore,

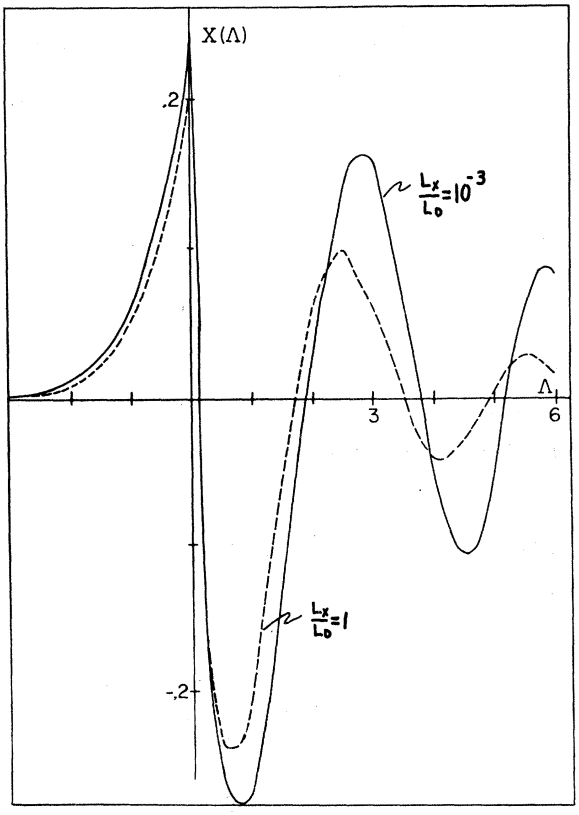

FIG. 1. Line-shape function $X(\Lambda)$.

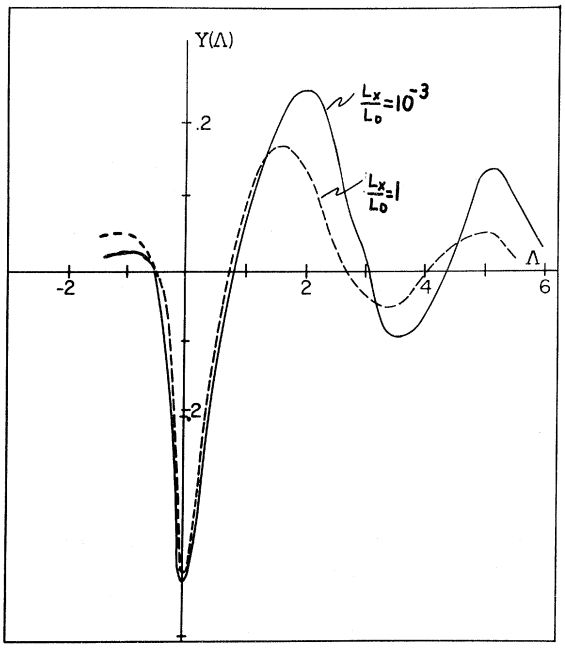

FIG. 2. Line-shape function $Y(\Lambda)$.

although the location of peaks and zero crossings on the axis depends on $\mathcal{E}_0$, the fact that the scale of the argument Λ is only dependent on $\mathcal{E}_0$ allows the horizontal scales of X and Y to be adjusted to fit experiment (determining $\mathcal{E}_0$ to within a constant) after L_x/L_D has been independently determined according to (i), above. Thus, this model makes possible separate identification of changes in surface-field magnitude and field nonuniformity, which is not done explicitly in Ref. 5.

For values of $L_x/L_D \gtrsim 3$, the energy term in the denominator of the logarithm in (14) becomes important. Specification of this intraband term requires knowledge (or assumption) of the carrier effective mass. Avoiding this problem places an upper limit of ~3 on the ratio L_x/L_D, which can be fitted to experiment using this theory. Independent determination of the effective mass by some means would extend the range of L_x/L_D over which theory could be compared with experiment.

In the calculation of Ref. 5, the real and imaginary parts of the dielectric function are seen to interchange in the limit of very large inhomogeneity. In our calculation, the exact shape of X and Y for large L_x/L_D depends on the value chosen for the effective mass. However, in the limit of very large L_x/L_D, the principal features of the curves are suppression of the peaks at $\Lambda = 0$ for both X and Y, relative growth of the first negative peak in X and the positive peak at $\Lambda < 0$ in Y with respect to all other peaks, and rapid quenching of satellite peaks. This theory therefore yields a mixing of real and imaginary parts of the dielectric function qualitatively similar to that found in Ref. 5 for very large inhomogeneities.

The experiment described below will be seen to fall within the range of field nonuniformities describable using our theory, namely, field penetrations small compared with λ but large enough to satisfy $L_x/L_D \lesssim 3$.

III. EXPERIMENTAL

Since λ_p will affect the experimentally determined $\delta\epsilon_1$ and $\delta\epsilon_2$ spectra, an experiment to test the theory must provide for its determination. Modulated ellipsometry provides measurements of $\delta\epsilon_1$ and $\delta\epsilon_2$. Also, as pointed out in Ref. 15, in the act of taking modulated-ellipsometry data, one also obtains an oblique-incidence electroreflectance spectrum. Thus, sufficient measurements are available to calculate λ_p from the experimental data, leaving only $\mathcal{E}_0$ and L_x/L_D as parameters to be adjusted in the curve-fitting process outlined in Sec. II.

The transition at 2.1 eV in Ge is known to give a strong electroreflectance structure, and has been chosen for an experimental illustration of the theory. Photoexcitation of another transition at the fundamental gap in Ge will increase the free-carrier density, changing $\mathcal{E}_0$ and L_x/L_D. These changes should appear as different values of $\mathcal{E}_0$ and L_x/L_D necessary for fitting the theory to the measured results.

The arrangement of the apparatus is shown schematically in Fig. 3. Except for the additional test-cell window to admit the photoexciting beam and the photoexciting beam source, the experiment is similar to ellipsometric techniques for measurement of $\delta\epsilon_1$, $\delta\epsilon_2$, and λ_p reported elsewhere in the literature.[11,15,16] Schmidt and Knausenberger[17] have employed a similar experimental arrangement, but have not extracted a value for λ_p from their results, or used photoexcitation to change the surface-field profile. Acquisition and analysis of the data follows the procedure of Refs. 4, 11, 15, and 16.

The samples are thin wafers of 30-Ω cm n-type Ge. The modulating field is applied by means of a voltage between the sample and at a Pt counter-

TABLE I. Relationship of $X(\Lambda)$ and $Y(\Lambda)$ to $\delta\epsilon_1$ and $\delta\epsilon_2$ for the various transition types.

Transition type	Λ[a]	$\delta\epsilon_1$	$\delta\epsilon_2$
M_0	$\frac{\hbar\omega - E_g}{\hbar\Omega}$	$\lvert\Omega\rvert^{1/2}Y(\Lambda)$	$\lvert\Omega\rvert^{1/2}X(\Lambda)$
M_1—transverse		$-\lvert\Omega\rvert^{1/2}X(\Lambda)$	$\lvert\Omega\rvert^{1/2}Y(\Lambda)$
M_1—parallel		$\lvert\Omega\rvert^{1/2}Y(-\Lambda)$	$-\lvert\Omega\rvert^{1/2}X(-\Lambda)$
M_2—transverse		$\lvert\Omega\rvert^{1/2}X(-\Lambda)$	$\lvert\Omega\rvert^{1/2}Y(-\Lambda)$
M_2—parallel		$-\lvert\Omega\rvert^{1/2}Y(\Lambda)$	$-\lvert\Omega\rvert^{1/2}X(\Lambda)$
M_3		$-\lvert\Omega\rvert^{1/2}Y(-\Lambda)$	$\lvert\Omega\rvert^{1/2}X(-\Lambda)$

[a] E_g is the energy gap.

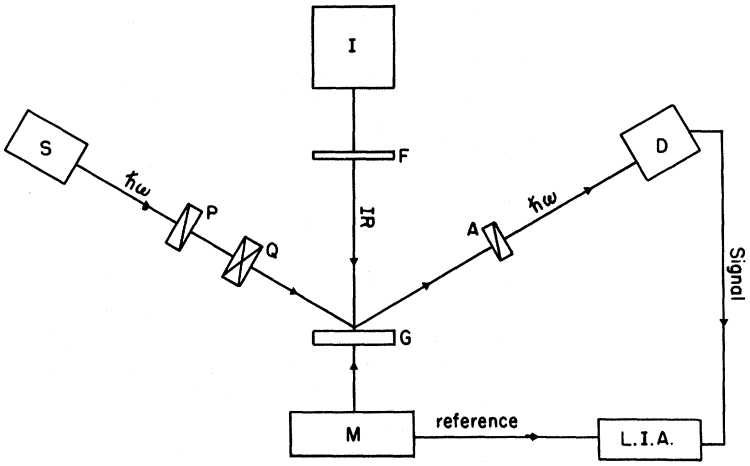

FIG. 3. Schematic diagram of the experiment: S, light source and monochromator; P, polarizer; Q, compensator; G, sample; F, infrared transmitting filter; I, tungsten light source; A, analyzer; M, modulating voltage source, ac plus dc bias; D, phototube; L. I. A., lock-in-amplifier.

electrode, both of which are immersed in a 1N KCl electrolyte. Conditions for modulation in one direction from the flat-band condition,[18] and for avoidance of surface contamination are determined using the procedure of Ref. 11, and employed throughout the subsequent experiments. Under these conditions, the experimental signals are due to changes in ϵ_1 and ϵ_2 in the space $0 \leq x \leq \lambda_p$ as the modulating electric field is turned on, and the results can be compared with the theory.

The photoexciting beam is just the output of a tungsten projection lamp, filtered to eliminate wavelengths shorter than 7500 Å, and focused to a spot about 2 cm^2 in area on the sample surface. The 7500-Å short-wavelength cutoff prevents excitation of the 2.1–2.3-eV transitions by this beam, but allows generation of electron-hole pairs across the fundamental gap in the Ge. The lamp current, and hence the beam intensity, are preset. Data are taken point by point, at 50-Å wavelength intervals over the photon energy range of interest.

IV. RESULTS AND DISCUSSION

Spectra of $\delta\epsilon_2$ vs $\hbar\omega$, with and without illumination by the second light beam, are shown in Fig. 4. Also shown are the results of fitting theory to experiment using the ratio of peak heights to determine L_x/L_D, and the location of zero crossings to determine the relative change in $\mathcal{E}_0$ under illumination. Similar spectra for $\delta\epsilon_1$ are shown in Fig. 5, together with the corresponding theoretical curves.

Although causality relates $\delta\epsilon_1$ and $\delta\epsilon_2$, the relationship occurs through an integral over all photon energies. Hence, the nearness of the spin-

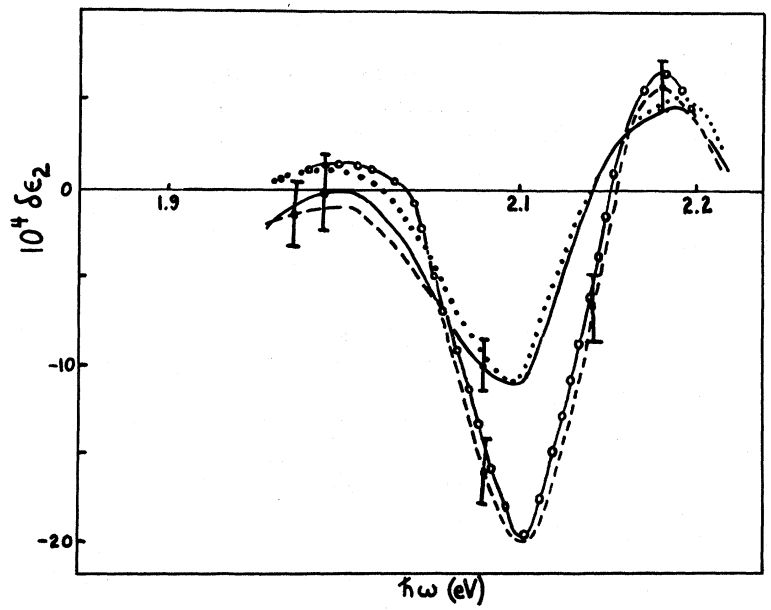

FIG. 4. Spectra of $\delta\epsilon_2$ vs $\hbar\omega$: solid line—experiment, no illumination; dotted line—theory, $L_x = 4000$ Å, $\mathcal{E}_0 = 1$ arbitrary unit; dashed line—experiment, with illumination; circles—theory, $L_x = 200$ Å, $\mathcal{E}_0 = 11$ arbitrary units.

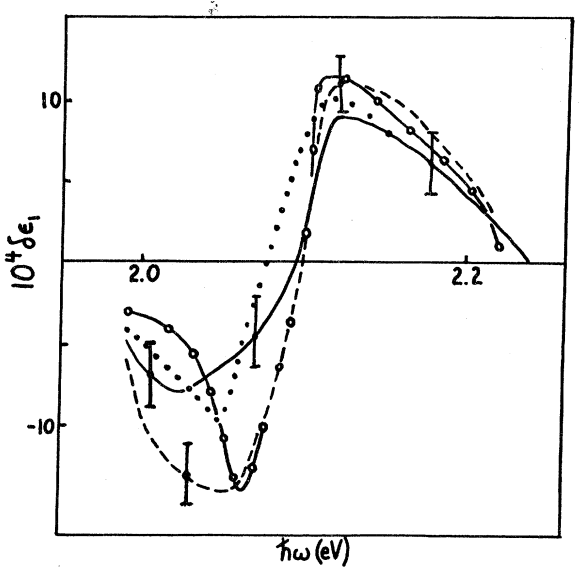

FIG. 5. Spectra of $\delta\epsilon_1$ vs $\hbar\omega$: solid line—experiment, no illumination; dotted line—theory, $L_x = 4000$ Å, $\mathcal{E}_0 = 1$ arbitrary unit; dashed line—experiment, with illumination; circles—theory, $L_x = 200$ Å, $\mathcal{E}_0 = 11$ arbitrary units.

orbit-split component of this transition at 2.3 eV suggests that an independent experimental determination of $\delta\epsilon_1$, as is possible with the modulated ellipsometric technique, might serve as a check on integration error because of the overlap of these two spectra. The fact that the best fit is obtained for both $\delta\epsilon_2$ and $\delta\epsilon_1$ independently, with the same values of $\mathcal{E}_0$ and L_x/L_D, indicates that overlap from the 2.3-eV spectra is not significant in this case.

In order to compute the penetration depth of the electric field from our results for L_x/L_D, a value for L_x must be assigned. This is not an additional adjustable parameter, but one which can be calculated from the available experimental data. For their study of electroreflectance near the fundamental gap, Aspnes and Frova[5] have used a penetration depth of

$$L_x = \lambda/(2\pi|(n_2 - n_1)|) , \tag{17}$$

where n_2 and n_1 are the refractive indices of the sample and ambient medium, respectively. For that case, which corresponds to L_D and $\lambda_p \gg \lambda$, the photon penetration depth is clearly limited by the momentum uncertainty principle applied to the change in photon momentum at the front sample surface, and (17) is a good estimate of L_x.

For our case, since $\lambda_p \ll \lambda$, the fact that the modulated region of the solid is a thin film of thickness λ_p must be taken into account, since reflected photons can come from any depth at which the optical properties remain different from those of the bulk.

A third possibility arises for the case of very strongly absorbing materials where essentially all of the photons are absorbed in a distance less than λ_p. In such materials the depth of the solid which is sampled by the reflected photons is just the inverse of the optical absorption coefficient.

In each of the three possibilities above, the modulated ellipsometry experiment provides sufficient data to obtain an experimental estimate of L_x. The wavelength is always known, and our experiment yields both λ_p and the absorption coefficient.

For the Ge samples studied, λ_p and the absorption distance are both approximately 400 Å, so it is not possible to identify the mechanism which limits the depth to which the light samples the optical properties of the solid. As long as L_x can be determined, however, this problem is not important.

If we assign $L_x = 400$ Å, we obtain L_D values of 4000 Å without illumination and 200 Å with illumination, a decrease of a factor of 20. If used as Debye lengths, these values give reasonable carrier densities in each case. The surface field $\mathcal{E}_0$ increases by a factor of 11, but not by an amount corresponding to the decrease in field penetration depth. This simply means that as the surface field increases, other parts of the experimental cell are taking up more of the total potential drop between the electrodes. This is to be expected since we have increased the conductivity of the Ge electrode by illuminating it.

The parameter λ_p does not appear to be sensitive to illumination over the range of light intensities available in this experiment. As pointed out earlier, λ_p cannot be expected to follow L_D in linear fashion. Also, since the plane $x = \lambda_p$ is illuminated very weakly because of absorption, it is not likely that changes in λ_p could be detected in this experiment very easily.

In summary, the experiment shows that, for our samples, the values of $\delta\epsilon_1$, $\delta\epsilon_2$, λ_p, and L_D are such that the WKB approximation of Ref. 5 would not be valid, and that the theory presented describes well the changes in surface field and field penetration depth as well as the changes in the line shapes of $\delta\epsilon_1$ and $\delta\epsilon_2$ that occur upon illumination of the sample with a second light beam.

V. CONCLUSION

We have shown that, in assessing the validity of approximations involving electroreflectance in a nonuniform field, four lengths characteristic of the problem are important. The relationship of λ and λ_p determines if the small-wave-number approximation is appropriate. The relative values of λ_p and the inverse absorption coefficient determine whether reflection from the front surface only, reflection from the modulated "surface film" $0 \leq x \leq \lambda_p$, or absorption dominate in determining the depth

in the sample from which the reflected light can return. Finally, the ratio L_x/L_D can greatly alter the line shapes of $\delta\epsilon_1$ and $\delta\epsilon_2$.

We have derived line shapes of $\delta\epsilon_1$ and $\delta\epsilon_2$ for an exponential model of the electric field, under the assumption that the field penetration depth and the depth to which the optical properties are modulated are smaller than the light wavelength. This approximation complements that of Aspnes and Frova,[5] which is valid when these depths are much larger than the light wavelength. As expected, and evident from Figs. 1 and 2, our theory approaches theirs as the field penetration depth becomes large compared with the photon penetration depth.

Using a modulated ellipsometry experiment which determines the values of λ_p and L_x directly, we have determined the electric field penetration depth, L_D and the line shapes of $\delta\epsilon_1$ and $\delta\epsilon_2$, and the relative change of $\mathcal{E}_0$ upon illumination of the sample with a second light beam. The fit of theory to experiment is excellent considering that all broadening mechanisms are neglected in the theory, and the fit yields reasonable values of the field penetration depth.

Modulated ellipsometry is too complicated an experiment, and the spectral range of ellipsometer components are too limited, for it to be a tool of general use in obtaining photoreflectance or electroreflectance spectra. It is, however, useful as a preparatory experiment, to determine the degree of field inhomogeneity that must be taken into account in the analysis of these spectra. Koeppen and Handler[19] have proposed optimum sample doping as a method for minimizing field inhomogeneity. An experiment such as this one would provide an experimental check on the success of such a method.

APPENDIX

We wish to calculate the eigenfunctions and eigenvalues for electrons in a solid in an electric field of the form $\mathcal{E} = \mathcal{E}_0 e^{-\alpha x}$. The potential has the form

$$f(x) = B(1 - e^{-\alpha x}) , \tag{A1}$$

where $B = -e\,\mathcal{E}_0/\alpha$, inside the solid.

The Schrödinger equation can be written

$$\left(-\frac{\hbar^2}{2m}\nabla^2 + V(\vec{r}) + f(x)\right)\phi_{\nu,n}(\vec{k},\vec{r}) = W_{\nu,n}(\vec{k}_\perp)\,\phi_{\nu,n}(\vec{k},\vec{r}) , \tag{A2}$$

where W is the eigenvalue in the presence of the field, $V(\vec{r})$ is the potential of the solid, including surface effects, in the absence of the applied field, and all other quantities have their usual meaning. We seek an expansion of the form

$$\phi_{\nu,n}(\vec{k},\vec{r}) = \sum_{k_x} A_{\nu,n}(\vec{k})\,\psi_n(\vec{k},\vec{r}) , \tag{A3}$$

where the ψ are the unperturbed eigenfunctions. Substituting (A3) into (A2) and taking the inner product with $\psi_{n'}(\vec{k}',\vec{r})$ yields

$$\sum_{k_x}\{A_{\nu,n}(\vec{k})\,[E_n(\vec{k}) - W_{\nu,n}(\vec{k}_\perp)]\delta_{nn'}\,\delta_{kk'} + A_{\nu,n}(\vec{k})\,\langle\psi_{n'}(\vec{k},\vec{r})\,|f(x)\,|\psi_n(\vec{k},\vec{r})\rangle\} = 0 . \tag{A4}$$

Using (A1) to evaluate the matrix elements of $f(x)$, we obtain

$$\langle\psi_{n'}(\vec{k},\vec{r})\,|f(x)\,|\psi_n(\vec{k},\vec{r})\rangle = B\delta_{kk'}\,\delta_{nn'} - B\,\exp\left[-i\alpha\left(\delta_{kk'}\,X_{nn'}(\vec{k}) - \delta_{nn'}\,\frac{\partial}{\partial k_x}\,\delta_{kk'}\right)\right] , \tag{A5}$$

where

$$X_{nn'}(\vec{k}) = \int_v d^3r\;\psi_{n'}^*(\vec{k},\vec{r})\,\frac{\partial}{\partial k_x}\,\psi_n(\vec{k},\vec{r}).$$

The off-diagonal terms of $X_{nn'}$ commute with the operator

$$\delta_{nn'}\,\frac{\partial}{\partial k_x}\,\delta_{kk'} .$$

Also, if we consider k to be continuous, the derivative the Kronecker δ is equivalent to the negative derivative of the function multiplying the Kronecker δ within the summation operation, over the variable of integration. Thus,

$$\langle\psi_{nn'}(\vec{k}',\vec{r})\,|f(x)\,|\psi_{nn}(\vec{k},\vec{r})\rangle = B\delta_{n'n}\,\delta_{kk'} - B\,\exp\left\{-i\alpha\left[\bar{X}_{nn'}(\vec{k}) + \delta_{nn'}\,\delta_{kk'}\left(\frac{\partial}{\partial k_x} + X_{nn}(\vec{k})\right)\right]\right\} , \tag{A6}$$

where we have defined

$$\bar{X}_{nn'}(\vec{k}) = X_{nn'}(\vec{k}) \quad \text{if } n \neq n'$$
$$= 0 \qquad\quad \text{if } n = n' .$$

Substituting (A6) into (A4) and rearranging terms yields

$$B\,\exp\left[-i\alpha\left(\frac{\partial}{\partial k_x} + X_{nn}(\vec{k})\right)\right]A_{\nu n}(k) = e^{i\alpha\,\delta_{\vec{k}\vec{k}'}\,\bar{X}_{nn'}(\vec{k})}\,[E_n(\vec{k}) - W_{\nu,n}(\vec{k}_\perp) + B]A_{\nu,n}(\vec{k}) . \tag{A7}$$

Equation (A7) can be solved in a form similar to that used by Argyres.[20] The result, which can now be substituted into (1), is

$$A_{\nu,n}(\vec{k}) = C_{\nu,n}(\vec{k}) \times \exp\left\{\frac{i}{\alpha}\left[\int_0^{k_x}\left(\ln\frac{1}{B}[E_n(\vec{k}_\perp,k_x') - W_{\nu,n}(\vec{k}_\perp) + B]\right)dk_x'\right.\right.$$

$$+\int_0^{k_x}\left[\delta_{kk'}X_{nn'}(\vec{k})-X_{nn}(\vec{k})\right]dk_x'\Bigg]\Bigg\}\,, \quad \text{(A8)}$$

where the eigenvalues $W_{\nu,n}$ remain to be found. The $C_{\nu,n}(\vec{k}_\perp)$ are just normalization constants.[6]

Imposing the condition of periodicity in k space leads to

$$\int_0^{K_x}\ln\left(\frac{1}{B}\left[E_n(\vec{k}_\perp,k_x')-W_{\nu,n}(\vec{k}_\perp)+B\right]\right)dk_x'+\Delta(\vec{k}_\perp,K_x) = -2\pi\alpha\nu\,, \quad \text{(A9)}$$

where ν is a positive integer and Δ has been defined in (4). Using (4) we can carry out the integration in (A9), solution of which yields the following equation for the eigenvalues:

$$W_{\nu,n}(\vec{k}_\perp)=\overline{E}_n(\vec{k})B-Be^{\theta}e^{-2\pi\nu\alpha/K_x}\,, \quad \text{(A10)}$$

where

$$\theta=2\left[1-\left(\frac{a}{x}\right)\tan^{-1}\left(\frac{x}{a}\right)\right]-\frac{1}{k_x}\Delta(\vec{k}_\perp,K_x)\,,$$
$$a^2=E_n(\vec{k}_\perp)-W_{\nu,n}(\vec{k}_\perp)+B\,, \quad \text{(A11)}$$
$$x^2=\hbar^2k_x^2/2\mu_x\,.$$

The quantity θ' used in Eq. (3) is obtained from (A11) by letting $k_x\to k_x'$.

*Present address: Engineered Systems Inc., Omaha, Neb. 68127.

[1]F. Evangelisti and A. Frova, Solid State Commun. 6, 621 (1968).
[2]A. Frova and D. E. Aspnes, Phys. Rev. 182, 795 (1969).
[3]B. O. Seraphin and N. Bottka, Solid State Commun. 7, 497 (1969).
[4]A. B. Buckman and N. M. Bashara, Phys. Rev. 174, 719 (1968).
[5]D. E. Aspnes and A. Frova, Solid State Commun. 7, 155 (1969).
[6]D. E. Aspnes, P. Handler, and D. F. Blossey, Phys. Rev. 166, 921 (1968).
[7]D. E. Aspnes, Phys. Rev. 147, 554 (1966).
[8]R. Jacobsson, Progr. Opt. 5, 247 (1965).
[9]P. Drude, Wied Ann. 43, 26 (1891).
[10]L. Rayleigh, Proc. Roy. Soc. (London) A86, 207 (1912).
[11]A. B. Buckman, J. Opt. Soc. Am. 60, 416 (1970).
[12]F. Cerdiera and M. Cardona, Solid State Commun. 7, 879 (1969).
[13]R. E. Nahory and J. L. Shay, Phys. Rev. Letters 21, 1569 (1968).
[14]D. E. Aspnes, Solid State Commun. 8, 267 (1970).
[15]A. B. Buckman, Surface Sci. 16, 193 (1969).
[16]A. B. Buckman and N. M. Bashara, J. Opt. Soc. Am. 58, 700 (1968).
[17]E. Schmidt and W. H. Knausenberger, J. Opt. Soc. Am. 59, 857 (1969).
[18]Y. Hamakawa, P. Handler, and F. A. Germano, Phys. Rev. 167, 709 (1968).
[19]S. Koeppen and P. Handler, Phys. Rev. 187, 1182 (1969).
[20]P. N. Argyres, Phys. Rev. 126, 1386 (1962).

PHYSICAL REVIEW B VOLUME 5, NUMBER 6 15 MARCH 1972

Shubnikov-de Haas Measurements in $Pb_{1-x}Sn_xSe$†*

John Melngailis, T. C. Harman, and W. C. Kernan
Lincoln Laboratory, Massachusetts Institute of Technology, Lexington, Massachusetts 02173
(Received 19 November 1971)

Oscillatory magnetoresistance measurements have been made on n- and p-type $Pb_{1-x}Sn_xSe$ with $x=0.08$, 0.17, and 0.20, and carrier densities between 2×10^{17} and 3×10^{18} cm^{-3}. The Fermi surface is made up of pockets of holes or electrons at the L point on the Brillouin-zone face. For n- and p-type samples with $x=0.17$ and 0.20 the Fermi surface is nearly spherical. For $x=0.08$ and 1.4×10^{18} holes/cm^3, clear anisotropy is seen corresponding to $K=1.71\pm0.1$. Cyclotron masses at the Fermi level were obtained. At the same carrier density, hole and electron masses appear equal, within the 10% accuracy of the measurements, indicating mirror bands. At high magnetic fields (up to 150 kG) spin splitting was observed and values for the g factors deduced. Expressions for the effective masses and g factors are derived from an existing six-band model and compared with the results.

I. INTRODUCTION

$Pb_{1-x}Sn_xSe$ is a semiconducting alloy with an energy gap dependent on composition x.[1,2] It has the NaCl crystal structure for $x<0.43$ (for $x>0.43$ the structure is that of SnSe, orthorhombic B29). As in the PbTe-SnTe alloys,[3] the addition of SnSe to PbSe decreases the energy gap of the material. At a composition $x=0.15$ (at 4.2 °K) the gap passes through zero and the conduction and valence bands